Synthesis of Hierarchical Self-Assembled $BaMoO_4$ Microcrystals

Eun-Kyoung Ryu and Young-Duk Huh*

*Department of Chemistry, Dankook University, Gyeonggi 448-701, Korea. *E-mail: ydhuh@dankook.ac.kr*

Received November 27, 2007

Key Words : Hierarchical self-assembly, Morphology, $BaMoO_4$

Hierarchical microstructures with specific morphologies have attracted great interest because of their novel properties and applications.[1-3] In general, hierarchical microstructures have been synthesized by using template precursors such as surfactant micelles, copolymer aggregates, and microemulsion droplets.[4-9] $BaMoO_4$ is widely used as a photoluminescence material and as a frequency shifter in stimulated Raman scattering.[10,11] $BaMoO_4$ is typically prepared with conventional solid-state reactions and microwave-assisted methods.[12,13] $BaMoO_4$ crystals with various morphologies such as nanobelts, nanofibers, and nanobrushes have recently been synthesized by using catanionic reverse micelles.[14-16] Hierarchical dendrites of $BaMoO_4$ have been prepared with a microemulsion method.[17] In this article, we report a simple precipitation method for preparing hierarchical self-assembled $BaMoO_4$ crystals by using N,N,N',N'-tetramethylethylenediamine (TMEDA) as a structure-directing agent. Single $BaMoO_4$ octahedral crystals were also prepared with a microemulsion method. The evolution of the morphology of the $BaMoO_4$ crystals from octahedral to hierarchical self-assembled was also examined.

Experimental Section

$Ba(NO_3)_2$ (Junsei), $Na_2MoO_4{\cdot}2H_2O$ (Aldrich), cetyltrimethylammonium bromide (CTAB, TCI), and TMEDA (TCI) were used as received. In a typical synthesis of hierarchical self-assembled $BaMoO_4$ crystals with the simple precipitation method, 30 mL of 0.08 M $Ba(NO_3)_2$ aqueous solution was added to 30 mL of 0.08 M $Na_2MoO_4{\cdot}2H_2O$ aqueous solution under stirring for 10 min. The reaction mixture was then incubated for 50 min at room temperature. To examine the effects of varying the molar ratio of [MoO_4^{2-}] to [Ba^{2-}], various concentrations of $Na_2MoO_4{\cdot}2H_2O$ were used for a fixed concentration of $Ba(NO_3)_2$ of 0.08 M. To investigate the effects of varying the TMEDA concentration, aqueous solutions were prepared by adding TMEDA (5 mM, 20 mM, 40 mM, 60 mM, or 80 mM) into the reaction mixture. $BaMoO_4$ crystals were also prepared by using a CTAB/water/cyclohexane/*n*-butanol microemulsion system. 2 mL of 0.1 M $Ba(NO_3)_2$ aqueous solution was added to a solution containing 4 g of CTAB, 40 mL of cyclohexane, and 8 mL of *n*-butanol, under vigorous stirring. A $Na_2MoO_4{\cdot}2H_2O$ microemulsion was also prepared. The two optically transparent solutions were mixed, and then incubated for 24 h at room temperature. To investigate the effects of varying the molar ratio w of H_2O to CTAB, various amounts of CTAB were used with other conditions fixed. Various w values of 5, 10, 15, and 20 were investigated. When w is higher than 20, the transparent microemulsion solution can not be obtained. The products were centrifuged and washed with water and ethanol several times, and then dried at 60 °C.

The structures of the as-prepared $BaMoO_4$ products were analyzed by carrying out powder X-ray diffraction (XRD, PANalytical, X'pert-pro MPD) with Cu Kα radiation. The morphologies of the products were characterized with scanning electron microscopy (SEM, Hitachi S-4300) and transmission electron microscopy (TEM, JEOL JEM-3010). The Raman spectra of the products were obtained with a Raman spectrometer (HORIABA Jobin Yvon T64000) using radiation of 514.5 nm from an argon ion laser.

Results and Discussion

Figure 1 shows a typical XRD pattern of an as-prepared $BaMoO_4$ product. All the peaks correspond to those of tetragonal $BaMoO_4$ and match those in reported data (JCPDS 85-0586, a = 5.394 Å, and c = 12.02 Å). The Raman spectrum of an as-prepared $BaMoO_4$ product is shown in Figure 2. The Raman peak at 889.1 cm^{-1} was assigned to the symmetric stretching vibration mode ν_1 (A_g) of the MoO_4^{2-} group in the $BaMoO_4$ crystal. The peaks at 837.7 and 790.1 cm^{-1} correspond to the anti-symmetric stretching ν_3 (B_g) and ν_3 (E_g) vibration modes. The peaks at 359.4 and 324.5 cm^{-1} correspond to the anti-symmetric and symmetric ν_4 (B_g) and

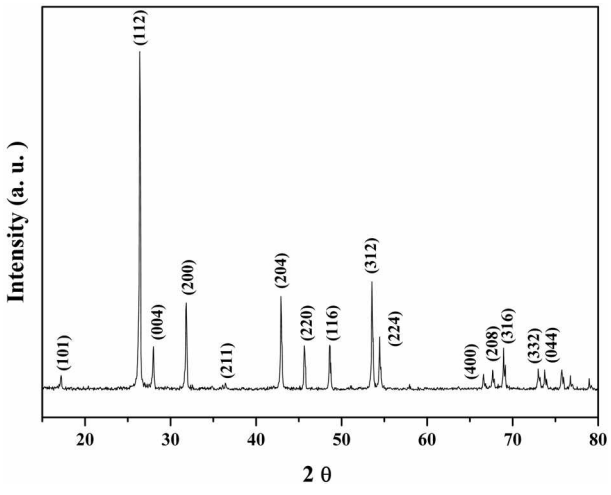

Figure 1. XRD pattern of an as-prepared $BaMoO_4$ product.

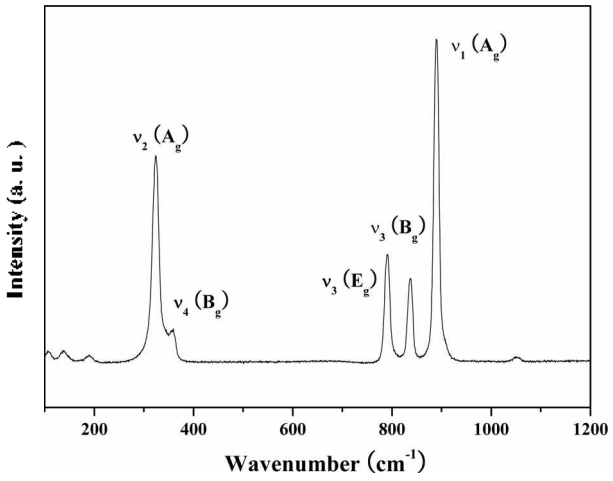

Figure 2. Raman spectrum of an as-prepared $BaMoO_4$ product.

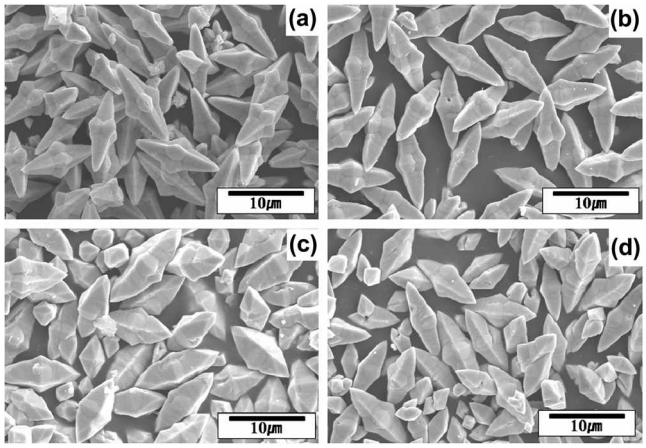

Figure 3. SEM images of the $BaMoO_4$ products obtained for various molar ratios of $[MoO_4^{2-}]$ to $[Ba^{2+}]$: (a) 0.1, (b) 0.25, (c) 0.5, and (d) 1.0.

ν_2 (A_g) bending modes respectively.[10] Since no peaks due to other impurities were detected in the XRD and Raman spectra, we conclude that $BaMoO_4$ was successfully synthesized.

Figure 3 shows SEM images of $BaMoO_4$ products obtained with the simple precipitation method for various molar ratios of $[MoO_4^{2-}]$ to $[Ba^{2+}]$. For $[MoO_4^{2-}]/[Ba^{2+}] = 0.1$, the $BaMoO_4$ crystals are composed of long central stems with four perpendicular branches, as shown in Figure 3(a). These crystals have an average length of about 10 μm. When $[MoO_4^{2-}]/[Ba^{2+}] = 1.0$, elongated bipyramid-like $BaMoO_4$ crystals were formed, as shown in Figure 3(d). As the molar ratio of $[MoO_4^{2-}]$ to $[Ba^{2-}]$ is increased, the sunken face of the bipyramid is filled. Since no surfactants or templates are used in this method, it is clear that the evolution of the morphology with increases in $[MoO_4^{2-}]/[Ba^{2+}]$ is a result of the pure crystal growth of the $BaMoO_4$ crystal.

Figure 4 shows SEM images of the $BaMoO_4$ products obtained with the simple precipitation reaction when various amounts of TMEDA were added for $[MoO_4^{2-}]/[Ba^{2-}] = 0.5$. When no TMEDA is used, a bipyramid-like morphology of

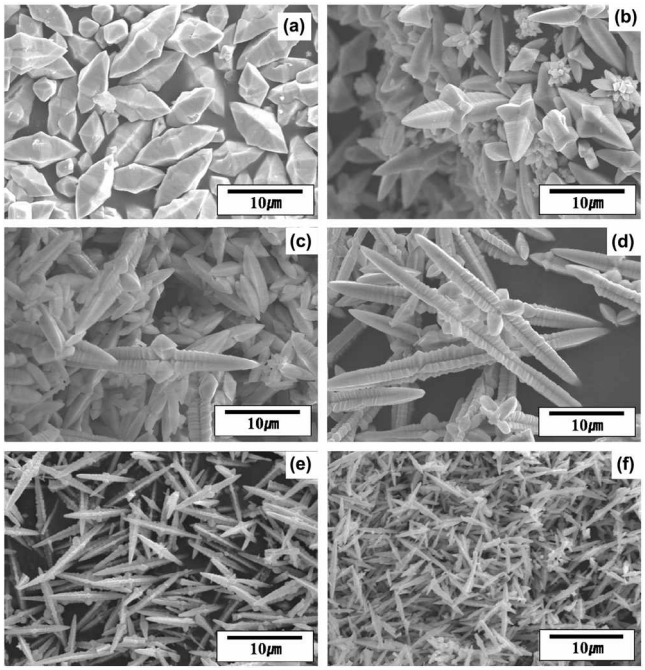

Figure 4. SEM images of $BaMoO_4$ products obtained for various amounts of added TMEDA at $[MoO_4^{2-}]/[Ba^{2+}] = 0.5$: (a) no TMEDA, (b) 5 mM, (c) 20 mM, (d) 40 mM, (e) 60 mM, and (f) 80 mM.

the $BaMoO_4$ products results, as shown in Figure 4(a), which is similar to the image in Figure 3(c). With increases in the amount of TMEDA, the size of the $BaMoO_4$ crystals increases. When 40 mM of TMEDA is used, the $BaMoO_4$ crystals have an average length of about 40 μm. These hierarchical self-assembled $BaMoO_4$ crystals are composed of very long central stems with four perpendicular branches, as shown in Figure 4(d). The cross-section of each stem looks like a star. Since the star-like cross-sections of the branches assemble face to face along the long central stem, grooves have formed in the stem. Four pyramid arms are also formed at the center of the long stem. Therefore, TMEDA was found to play an important role in the formation of hierarchical self-assembled $BaMoO_4$ crystals. TMEDA is a water-soluble and bidentate amine that can combine with Ba^{2+} to form the barium-amine complex $[Ba(TMEDA)_3]^{2+}$. This complex reacts with MoO_4^{2-} in solution to form $BaMoO_4$, in conjunction with the release of TMEDA. The possible chemical reactions producing $BaMoO_4$ are as follows:

$$Ba^{2-}\,(aq) + 3\ TMEDA \rightarrow [Ba(TMEDA)_3]^{2+}\,(aq) \qquad (1)$$

$$[Ba(TMEDA)_3]^{2+}\,(aq) + MoO_4^{2-}\,(aq) \rightarrow BaMoO_4\,(s) + 3\ TMEDA \qquad (2)$$

When no TMEDA is used, Ba^{2+} reacts directly with MoO_4^{2-} to form bipyramid-like $BaMoO_4$ crystals, as shown in Figure 3(d). There is insufficient time for self-assembled $BaMoO_4$ crystals to form in the absence of TMEDA. In contrast, hierarchical self-assembled $BaMoO_4$ crystals form for higher TMEDA concentrations, as shown in Figure 4(d).

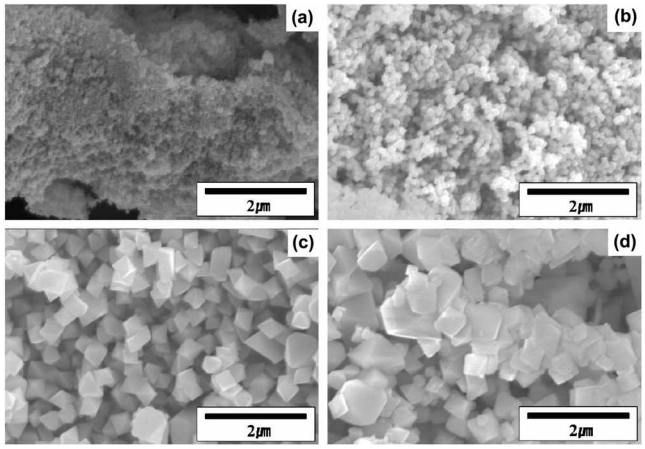

Figure 5. TEM images of the as-prepared $BaMoO_4$ crystals obtained for various values of w: (a) 5, (b) 10, (c) 15, and (d) 20.

TMEDA affects the rate of formation of the $BaMoO_4$ crystals. TMEDA reacts with Ba^{2-} to form the stable $[Ba(TMEDA)_3]^{2+}$ complex: the formation of this complex retards the overall reaction rate, and there is thus sufficient time for the assembly of a hierarchical structure of $BaMoO_4$ crystals of the longest with sizes up to 40 μm. Therefore, under these conditions hierarchical self-assembled crystals with a long central stem and four perpendicular branches appear due to the fast crystal growth along the direction of the stem. However, the size of $BaMoO_4$ crystal having similar hierarchical self-assembled external shape is decreased when the TMEDA concentration is higher than 40 mM. The average size of $BaMoO_4$ crystal is decreased to 7 μm at the highest TMEDA concentration of 80 mM, as shown in Figure 4(f). At these higher TMEDA concentrations, the rate of crystal growth of $BaMoO_4$ may be retarded by the TMEDA.

Figure 5 shows TEM images of the $BaMoO_4$ products obtained with the microemulsion method. The crystal growth of $BaMoO_4$ is hindered by addition of CTAB surfactant. We found that the size of the as-prepared $BaMoO_4$ crystals strongly depends on the value of w (the molar ratio of H_2O to CTAB); the concentration of CTAB was varied with other conditions fixed. As shown in Figure 5(a), the crystals are composed of particles with sizes less than 100 nm. However, for w = 15, uniform octahedral $BaMoO_4$ crystals with an average size of 350 nm were obtained, as shown in Figure 5(c). Therefore, the crystal size of the $BaMoO_4$ products increases with increases in w.

Figure 6 shows TEM images of $BaMoO_4$ products obtained for w = 10. Octahedral with an average size of 150 nm were obtained, as shown in Figure 6(a). Figure 6(c) shows a high-resolution TEM (HRTEM) image of an individual octahedral $BaMoO_4$ crystal. The observed lattice spacings of 0.316, 0.343, and 0.335 nm correspond to the (004), (103), and (112) planes of tetragonal $BaMoO_4$ crystals respectively. Figure 6(d) shows the fast Fourier transform (FFT) patterns corresponding to the lattice fringes.

In general, the shape of these crystals can be explained in terms of the growth rates along <001> and <100> (or <010>). For the octahedral crystals prepared with the micro-

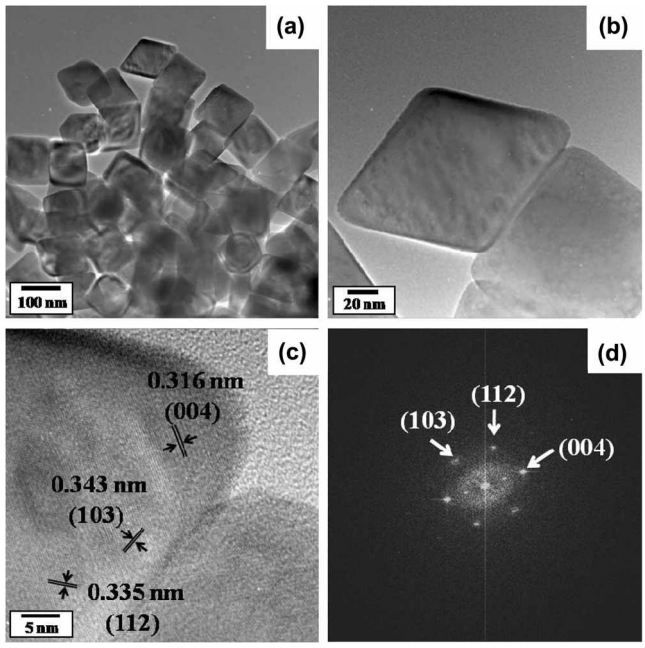

Figure 6. (a) and (b) TEM images of an individual octahedral $BaMoO_4$ crystal prepared at w = 10, (c) HRTEM image and (d) FFT pattern recorded from the edge of the octahedron.

emulsion method, the growth rate along <001> is equal to that along <100>. When the simple precipitation method was used, bipyramid-like crystals were obtained. For bipyramid-like crystals to form, the growth rate along <001> must be faster than that along <100>. As the concentration of TMEDA is increased, the morphology of the $BaMoO_4$ microcrystals varies from bipyramid-like to hierarchical self-assembled with a very long central stem and four perpendicular short branches. For hierarchical self-assembled crystals to form, the growth rate along <001> must be much faster than that along <100>. Crystal growth along <001> is preferred at higher TMEDA concentrations up to 40 mM. Therefore, TMEDA plays an important role in determining

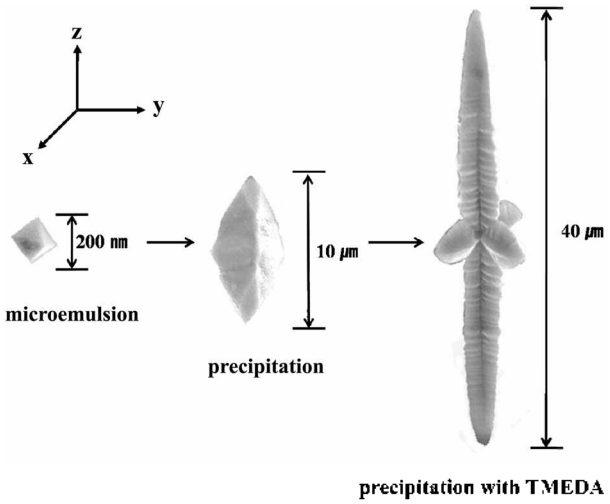

Figure 7. The various crystal morphologies: octahedral, bipyramid-like, and hierarchical self-assembled.

the shape of the hierarchical self-assembled $BaMoO_4$ crystals. Figure 7 shows a diagram of these changes in crystal morphology.

In conclusion, we have synthesized hierarchical self-assembled $BaMoO_4$ crystals with a long central stem and four perpendicular branches. As the concentration of TMEDA is increased up to 40 mM, the morphology of the $BaMoO_4$ crystals changes from bipyramidal to hierarchical self-assembled with an average size up to 40 μm. TMEDA plays an important role in determining the shape of the hierarchical self-assembled $BaMoO_4$ crystals. Nano-sized $BaMoO_4$ octahedra were also prepared with a microemulsion method. The evolution of the morphology of the $BaMoO_4$ crystals from octahedral to bipyramid-like to hierarchical self-assembled was investigated.

References

1. Antonietti, M.; Ozin, G. A. *Chem. Eur. J.* **2004**, *10*, 28.
2. Mann, S. *Angew. Chem. Int. Ed.* **2000**, *39*, 3392.
3. Song, H. C.; Park, S. H.; Huh, Y. D. *Bull. Kor. Chem. Soc.* **2007**, *28*, 477.
4. Gong, Q.; Qian, X.; Ma, X.; Zhu, Z. *Cryst. Growth Des.* **2006**, *6*, 1821.
5. Yu, S. H.; Antonietti, M.; Cölfen, H.; Hartmann, J. *Nano Lett.* **2003**, *3*, 379.
6. Yu, S. H.; Cölfen, H.; Antonietti, M. *J. Phys. Chem. B* **2003**, *107*, 7396.
7. Zhang, X.; Xie, Y.; Xu, F.; Tian, X. *J. Colloid Interface Sci.* **2004**, *274*, 118.
8. Liu, J.; Wu, Q.; Ding, Y. *Cryst. Growth Des.* **2005**, *5*, 445.
9. Cao, M.; Wu, X.; He, X.; Hu, C. *Langmuir* **2005**, *21*, 6093.
10. Basiev, T. T.; Sobol, A. A.; Voronko, Y. K.; Zverev, P. G. *Opt. Mater.* **2000**, *15*, 205.
11. Marques, A. P. A.; de Melo, D. M. A.; Longo, E.; Paskocimas, C. A.; Pizani, P. S.; Leite, E. R. *J. Solid State Chem.* **2005**, *178*, 2346.
12. Afanasiev, P. *Mater. Lett.* **2007**, *61*, 4622.
13. Ryu, J. H.; Yoon, J. W.; Lim, C. S.; Shim, K. B. *Mater. Res. Bull.* **2005**, *40*, 1468.
14. Li, Z.; Du, J.; Zhang, J.; Mu, T.; Gao, Y.; Han, B.; Chen, J.; Chen, J. *Mater. Lett.* **2005**, *59*, 64.
15. Shi, H.; Qi, L.; Ma, J.; Wu, N. *Adv. Funct. Mater.* **2005**, *15*, 442.
16. Zhang, C.; Shen, E.; Wang, E.; Kang, Z.; Gao, L.; Hu, C.; Xu, L. *Mater. Chem. Phys.* **2006**, *96*, 240.
17. Gong, Q.; Qian, X.; Cao, H.; Du, W.; Ma, X.; Mo, M. *J. Phys. Chem. B* **2006**, *110*, 19295.